Close Accord on Partial Discharge Diagnosis During Voltage Harmonics in Electric Motors Fed by Variable Frequency Drives

Waqar Hassan[1], Muhammad Akmal[2*], Ghulam Amjad Hussain[3], Ali Raza[4], and Muhammad Shafiq[5]

[1]Department of Electrical Engineering & Technology, Institute of Southern Punjab, Multan, Pakistan
[2]Department of Engineering & Mathematics, Sheffield Hallam University, Sheffield, S1 1WB, UK
[3]College of Engineering & Applied Sciences, American University of Kuwait, Kuwait
[4]Department of Electrical Engineering, University of Engineering and Technology, Lahore, Pakistan
[5]Department of Electrical Power Engineering and Mechatronics, Tallinn University of Technology, Estonia
[*]m.akmal@shu.ac.uk

***Abstract*—Partial discharge (PD) diagnostics test is reliable for estimating insulation health conditions in power system components. During laboratory PD diagnostics, the effect of harmonic components in the voltage waveform generated by variable frequency drives (VFD) fed electric motors (EMs) is often overlooked. However, these harmonic components can cause significant distortion in the applied voltage waveform. As VFD-fed EMs operate at low speeds, the harmonic concentration in the voltage increases. It has been found that PD activity in VFD-fed EM is significantly affected by the addition of harmonic components in the voltage, thus making it necessary to consider their impact when performing true PD diagnostics. This paper investigates the influence of voltage harmonic distortion produced in VFD-fed EM on PD severity and the subsequent insulation degradation. Eight VFD-fed EM are used to study PD behavior under different levels of harmonic pollution. The PD characteristics, such as inception voltage, pulse repetition rate, accumulated apparent charge, average discharge current, discharge power, and quadratic rate, are determined. With the help of probability distribution functions, the chance of PD activity and its severity at various voltage harmonic levels are estimated. The proposed technique can be used to plan maintenance activities that ensure reliability for industrial applications dealing with voltage harmonic distortion.**

1. Introduction

The variable frequency drives (VFD) fed electric motors (EMs) are widely used in automotive, ship, aviation, and other industries due to their cost efficiency, reliable speed control, lightweight, high specific power, and energy-saving capabilities [1-3]. However, when VFD-fed EMs are in operation, the harmonic components in the applied voltage waveform may develop, which could lead to premature insulation failure of the stator winding over time [4]. Therefore, online condition monitoring of VFD-fed EMs is essential to detect any pre-emptive winding insulation failure and plan regular maintenance activities [5, 6].

Partial discharges (PD) diagnostics test is a reliable method for estimating the health of stator insulation when conducting online condition-based monitoring and offline evaluation of VFD-fed electric motors [7-9]. In laboratory-based studies, PD measurements are typically conducted using a sinusoidal waveform of the applied voltage. However, in field operations, variable speed operation of VFD-fed EM can produce several harmonic components, resulting in a distorted voltage waveform that can significantly affect PD activity in the winding insulation [5]. Therefore, a better understanding of harmonic distortion in the applied voltage waveform is essential for accurately assessing the severity of PD and establishing an effective maintenance scheduling strategy for stator insulation in EMs.

Previous studies have investigated the effects of VFD-fed EMs on PD behavior and insulation degradation of stator windings [10-12]. For instance, Almeida et al. investigated technical and non-technical barriers (e.g., power quality and reliability issues) associated with the broader applications of VFD-fed EMs [13]. Also, the possible technical solutions to improve the performance of VFD-fed EMs based systems are discussed. In [14], Billard et al. studied the PD activity in EMs fed by inverter using a non-intrusive electromagnetic sensor. Furthermore, the experimental results revealed that PD activity in the stator winding might lead to premature insulation failure. Florkowski et al. in [15] investigated the impact of harmonic pollution in the applied voltage waveform on PD behavior and pattern evolution. Based on the experiments, the author observed that the harmonic distortion in the applied voltage significantly impacts PD intensity and maximum charge. In [16], Bahadoorsingh et al. studied the insulation characteristics of epoxy resin under harmonic distortion in the applied voltage waveform. It is also examined that the growth of an electric tree due to voltage harmonic distortion ultimately shortens the lifetime of the insulation. Hassan et al. explored the effect of harmonic contents in the applied voltage produced during the variable speed operation of EM on PD activity [5]. Also, mathematical modeling has been carried out to develop relationships between distortion and discharge parameters. Montanari et al. performed a comparative study investigating the influence of multi-level inverter supply and pure sine wave voltage on PD activity [17]. Furthermore, the aging estimation of the insulation in twisted wire pairs is also presented.

In summary, the existing literature has already studied the effect of specific voltage harmonic components on PD behavior and winding insulation endurance in EM. However, there is a lack of knowledge about PD investigation under real harmonic regimes experienced during variable operating

conditions of VFD-fed EM. This paper fills this gap by presenting the PD behavior of VFD-fed EM under a real harmonic regime. Also, based on the experimental results, a method is proposed to establish the relationship between PD activity and severity with harmonic distortion produced in the VFD system.

This study presents an approach to measure PD activity and assess the impact of voltage harmonic distortion on PD severity in VFD-fed EM. For this purpose, eight VFD-fed EMs were tested with variable speed operation from 5% to 100%, resulting in voltage distortion up to 41.94% THD_V (total harmonic distortion in voltage) and 2.31 K_s (waveshape parameter). Online PD measurements are performed under different voltage harmonic distortions by detecting a PD sweep signal of 20 ms. From the detected PD signal, several PD characteristic features, including PD inception voltage (PDIV), pulse repetition rate (m), accumulated apparent charge (q_a), average discharge current (I), discharge power (P), and quadratic rate (D), are evaluated. At a different level of harmonic distortion, the probability distribution functions of PD characteristic features are developed to infer statistical characteristics of PD data. With the help of an appropriate probability distribution function, the probability of PD activity and its severity at various voltage harmonic levels were estimated.

The rest of the paper is structured in the following way: Section II outlines the methodology used in this study. Section III explains the experimental setup, test object, and procedure for online PD measurement. In Section IV, the effects of variable speed operations of VFD-fed EM on voltage harmonics and modeling of the harmonic index are discussed. Section V presents the PD measurements and experimental results. Section VI provides the probability of PD activity and estimation of PD severity. Finally, Section VII summarizes the conclusions of this research.

2. METHODOLOGY

Fig. 1 illustrates the steps taken to investigate the influence of voltage harmonic distortion produced in VFD-fed EM on PD severity and the subsequent insulation degradation. The process is outlined as follows:

3. A 12-pulse VFD is used in the laboratory, and eight EMs are chosen for the experiment. A test bench for online PD measurement is set up to study the PD activity with different voltage harmonic distortion levels by recording the PD sweep signals of 20 ms. In [4], both the 5^{th} and 7^{th} harmonic components are generated during the operation of 12-pulse VFD. Additionally, the concentration of these harmonic components in the applied voltage waveform increases when the speed of VFD slows down. Therefore, a non-intrusive testing technique is used to evaluate the effect of variable speed operation of VFD-fed EMs on THDv and K_s of the applied voltage.
4. At different levels of THD_V and K_s of the applied voltage, online PD measurements in VFD-fed EMs are conducted, and various PD features are assessed, which can be used to determine the extent of PD under varying levels of harmonic distortion.

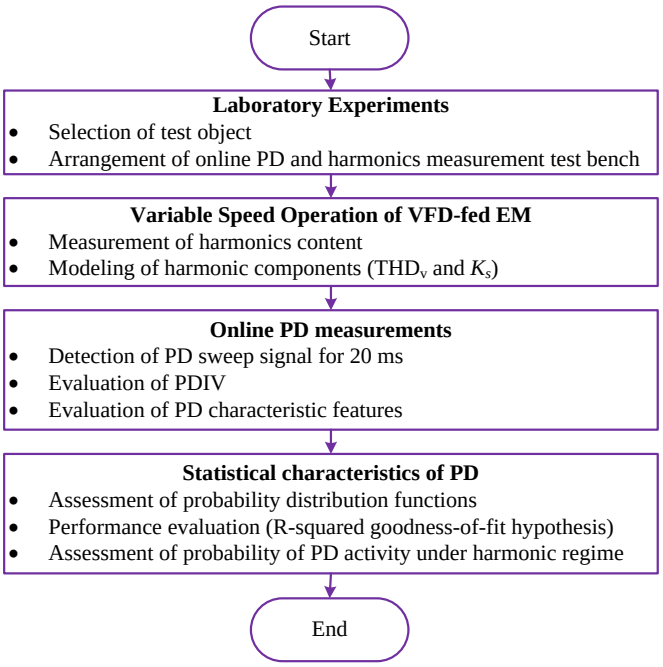

Fig. 1. *Methodology for analyzing the impact of voltage harmonic distortion on PD severity in VFD-fed EM*

5. Several probability distribution functions of PD characteristic features are evaluated to determine the statistical characteristics of PD data. Finally, the goodness-of-fit hypothesis is used to determine which probability distribution function best describes the probability of PD activity and associated severity level under various levels of voltage harmonic distortion.
6. This experimental work detected 350 PD sweep signals at different THD_V and K_s values of the applied voltage to obtain reliable results. This study is beneficial in demonstrating the PD activity under various levels of voltage harmonic distortion experienced by VFD-fed EMs during operation.

3. LABORATORY EXPERIMENTS

In this section, the setup of an online PD experiment in a laboratory environment, the selection of VFD-fed EMs as the test object, and the procedure for PD diagnostics are described.

Experimental Setup

This laboratory-based online PD experimental setup comprises a 15 kVA adjustable 3-phase AC power supply source (380 V to 690 V) connected to VFD-fed EM. The EM is connected to VFD via a 1-meter long 10 mm diameter single core flexible power cable. The voltage harmonics in the power supply source are carefully analyzed and found to be minimal (THD_V < 4%), making it effectively harmonic-free.

Fig. 2 presents the experimental setup (schematic diagram and physical image) established to conduct online PD measurements. A power quality analyzer is connected to VFD-fed EMs to assess the voltage harmonics during variable speed operations. A coupling capacitor (10 nF) is connected to one terminal of the VFD-fed EM, which served as a PD sensor and transferred the PD current pulses to the

quadrupole. The quadrupole then converted these current pulses into voltage signals, providing the PD voltage signal to the PD detector. A data acquisition device is connected to the PD detector, translating the analog PD signals into digital samples. The PD diagnostics tests are performed in accordance with the IEC 60034-27 Standard [9], adjusting the minimum values of linear error (less than 0.2 pC) and basic noise level (less than 0.1 dB). The calibration of the PD experimental test setup is carried out as per the IEC 60270 standard [18].

Specification of Test Object

In this experimental study, a total of eight identical EMs are used. Table 1 displays the details of both VFD and EMs.

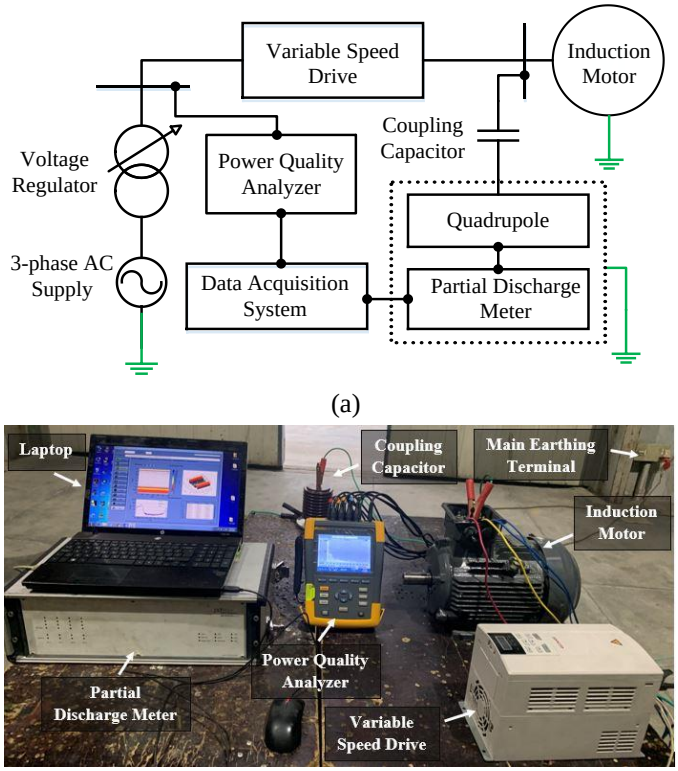

(a)

(b)

Fig. 2. (a) *Block diagram and* ***(b)*** *photograph show the experimental test setup developed in the laboratory for online PD diagnostics.*

Table 1 Detailed specifications of both VFD and EMs used in the PD diagnostics

Description	Specification
Variable frequency drive (VFD)	Rated voltage: 380 V to 690 V, 12 pulse, Rated power: 7.5 kW, No of phases: 3, Insulation Class: F (155 ^{o}C), Input frequency 50 Hz, output frequency: 5 – 50 Hz, Connection: delta, Brand: ABB
Induction motor	Rated voltage: 380 to 690 V, Rated power: 5 kW, No of phases: 3, Rated current: 9.2 A, Insulation Class: F (155 ^{o}C), No of poles: 4, Ingress protection (IP)-55, Power factor (cos θ): 0.85, Rated efficiency: 96%, Input frequency: 50 Hz, Connection: delta, Brand: ABB

PD Diagnostics Procedure

This research used a two-step process to estimate the PD severity and the calculation of PD characteristic parameters.

At first, the VFD is manually adjusted to set the operating speed of the EM at 100%. Based on our previous experimental results in [4], the THD_V calculated at this speed is approximately 4.5%, meeting the standards [19], and a nearly sinusoidal waveform of voltage was produced. To ensure thermal stability, the VFD-fed EM is operated at this speed for 10-15 minutes and the PDIV is examined by slowly increasing the applied voltage. Subsequently, the operating speed is adjusted in small decrements from 100% to 5%, and experiments are repeated to assess the PDIV at different speeds.

In the second step, the effects of voltage harmonic distortion generated by the variable speed operation of VFD-fed EM on PD activity are studied by assessing the PD characteristic features. For this purpose, a voltage equal to PDIV value detected during 100% operating speed, is applied to the VFD-fed EM and PD activity is examined at different speeds ranging from 5% to 100%. At each operating speed, the harmonic distortion in the applied voltage waveform is recorded, and PD measurements are performed.

Fig. 3 provides a visual representation of a typical applied voltage waveform with harmonic distortion (black line) and its corresponding PD signal at an operating speed of 41% and THD_V of 24.6%. The PD signal in Fig. 3(a) is shown as a blue line with its amplitude calibrated in mV, denoted by $V_{pd}(t_i)$. The same applied voltage waveform and PD signal in Fig. 3(b) is calibrated in nC, denoted by q_i. The q_i is determined as:

$$q_i = C \times V_{pd}(t_i) \quad (1)$$

In Eq. 1, C stands for the coupling capacitance and t_i is the sampling instant. With the PD signals obtained at different levels of voltage harmonics, several PD characteristic features such as q_a, m, I, P, and D can be determined to evaluate the impact of voltage harmonics distortion on the likelihood of PD activity in VFD-fed EM. The exact process for assessing PD characteristic features has already been outlined in [20].

4. EFFECT OF VARIABLE OPERATING CONDITIONS OF VFD-FED EM ON HARMONICS

The variable speed operation of VFD-fed EM lead to the production of voltage harmonics which have a substantial impact on the PD activity in the winding insulation. Therefore, it is essential to assess the level of voltage harmonic distortion in this type of EM prior to conducting PD diagnostics.

4.1. Variable Speed Operation of VFD-fed EMs

In the industries, the operation of EMs at variable load and speed helps to reduce power consumption. However, this causes a significant increase in voltage harmonics, which is quantified by THD_V [21]. Fig. 4 presents the relationship between THD_V and operating speed for eight VFD-fed EMs observed during the experiments. It can be seen that the lower the operating speed, the higher the THD_V level.

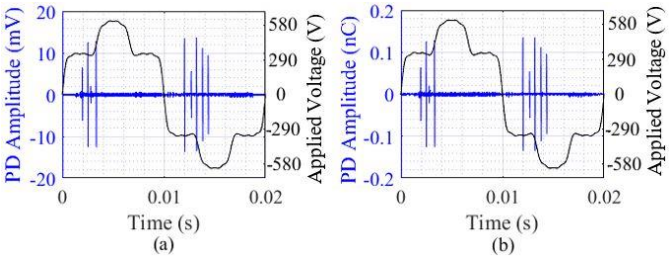

Fig. 3. *PD sweep signal recorded at 41% operation speed, with K_s = 1.73, and THD_V = 24.6%* ***(a)*** *$U_a(t_i)$ and $U_{pd}(t_i)$ in mV,* ***(b)*** *$U_a(t_i)$ and q_i in nC*

4.2. Modeling of Harmonic Distortion Index

Typically, the voltage harmonic distortion can be characterized using several parameters [16, 22]. These parameters include:

4.2.1 THD_V index: THD_V index is an important measure for assessing the harmonic distortion in the voltage waveform [4], which can be calculated using equation (2).

$$THD_V\ (\%) = \sqrt{\sum_{n=2}^{N}\left(\frac{V_n}{V_1}\right)^2} \times 100 \qquad (2)$$

where N represents the highest voltage harmonic order taken into account, n represents the specific voltage harmonic order, and V_n and V_1 are the rms values of n^{th} order of voltage harmonic components and the fundamental voltage, respectively.

4.2.2 Waveshape parameters (K_s and K_f): both K_s and K_f determine the steepness of the derivative of the resulting voltage waveform, which can contain harmonic distortion. The Fourier decomposition of this waveform is given by (3).

$$V(t) = \sum_{n=1}^{N} V_n \sin(n\omega_1 t + \psi_n) \qquad (3)$$

where ω_1 is the angular frequency of the sinusoidal voltage waveform and ψ_n is the phase shift of the concerned harmonic order. From (3), the slope of the waveform is given as:

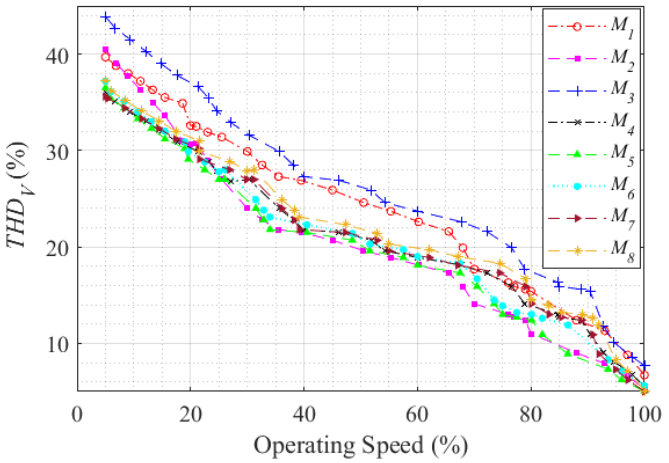

Fig. 4. *Relation between the speed ratio and THD_V for eight VFD-fed EMs (M-1 to M-8)*

$$\left(\frac{dV(t)}{dt}\right)_{rms} = \frac{\omega_1}{\sqrt{2}}\sqrt{\sum_{n=1}^{N} n^2 V_n^2} \qquad (4)$$

The slope of the fundamental applied voltage waveform is given as:

$$\left(\frac{dV}{dt}\right)_{rms} = \frac{\omega_1}{\sqrt{2}} V_1 \qquad (5)$$

The value of K_f is calculated by dividing (4) with rms values of the derivative of sinusoidal voltage waveform, with the same value of fundamental component in the distorted voltage waveform, as given by (6):

$$K_f = \sqrt{\sum_{n=1}^{N} n^2 \alpha_n^2} \qquad (6)$$

where

$$\alpha_n = \frac{V_n}{V_1} \qquad (7)$$

K_s is given by (8)

$$K_s = \frac{\omega_1}{\omega_0} \times K_f \qquad (8)$$

where ω_0 is the angular frequency of the fundamental voltage waveform and ω_1 is the angular frequency of 50 Hz voltage waveform. Also, the ratio of ω_1 and ω_0 is equal to 1, meaning that both equations (6) and (7) are the same since ω_0 is equal to 50 Hz.

4.2.3 Peak modification factor (K_p): K_p is also known as peak parameter, and is calculated as:

$$K_p = \frac{V_{np}}{V_{1p}} \qquad (9)$$

where V_{np} and V_{1p} represent the peak values of composite voltage waveform and fundamental voltage waveform, respectively.

4.2.4 RMS parameter (K_{rms}): K_{rms} is determined using (10):

$$K_{rms} = \frac{V_{nrms}}{V_{1rms}} \qquad (10)$$

where V_{nrms} and V_{1rms} represent the rms values of composite voltage waveform and fundamental voltage waveform, respectively. In this study, THD_V and K_s are utilized to analyze the harmonic distortion in the applied voltage waveform.

4.3. Investigation of Applied Voltage Waveform

When VFD-fed EMs is operated at different speeds, the applied voltage waveform is captured using power quality analyzer and harmonic components associated to a specific speed are modeled. It is observed that the decrease in the operating speed causes an increase in both THD_V and K_s, as witnessed in Fig. 5. From Fig. 5, when operating speed of EM is 100%, both THD_V and K_s are 4.61% and 1.27, respectively. By reducing the operating speed from 100% to 5%, both THD_V and K_s significantly raised up to 41.94% and 2.31,

respectively. For each voltage waveform, the test is successively performed for five minutes, and PD activity is investigated. To eliminate the effect of preceding voltage waveform, each successive test is performed without disconnecting the applied voltage source.

5. Experimental Results and Discussions

This section presents the PD measurements conducted online to evaluate the PDIV and PD characteristics under varying levels of voltage harmonic concentration.

5.1. Partial Discharge Inception Voltage (PDIV)

The PD activity is studied under different voltage harmonics by measuring the PDIV. For each THD_V level, the experiment is carried out 10 times and the average value of PDIV is calculated. The results of PDIV at different THD_V levels are displayed in Fig. 6. From Fig. 6(a), the presence of harmonic components in the applied voltage waveform can be seen to reduce the PDIV. This reduction is from 580 V to 460 V when THD_V and K_s levels are increased from 4.61% to 41.94% and 1.27 to 2.31, respectively. The normalized PDIV at a given THD_V level, represented by $U_{i,N}(THD_V)$, is then calculated to compare the value of PDIV reduced due to the presence of harmonic components in the applied voltage waveform, as expressed by (11).

$$U_{i,N}(THD_V) = \frac{U_i(THD_V)}{U_i(f)} \qquad (11)$$

where $U_i(THD_V)$ and $U_i(f)$ represent the average values of PDIV calculated at specific THD_V level and at reference THD_V level, respectively. Fig. 6(b) presents the results of normalization. From Fig. 6(b), it can be observed that the increase in THD_V level from from 4.61% to 41.94% causes to reduce the $U_{i,N}(THD_V)$ to 0.793.

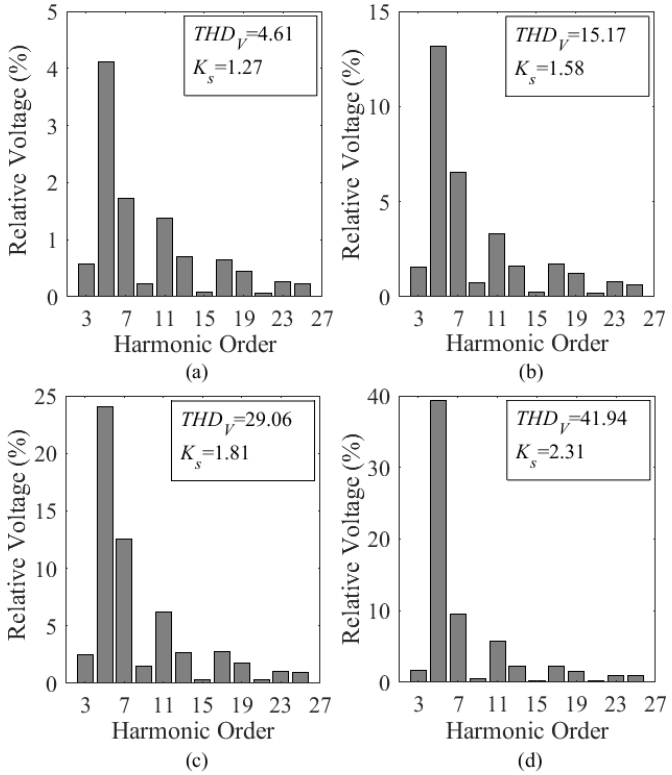

Fig. 5. *Harmonic spectrum of applied voltage waveform at an operating speed (a) 100%, (b) 71%, (c) 22%, and (d) 5%*

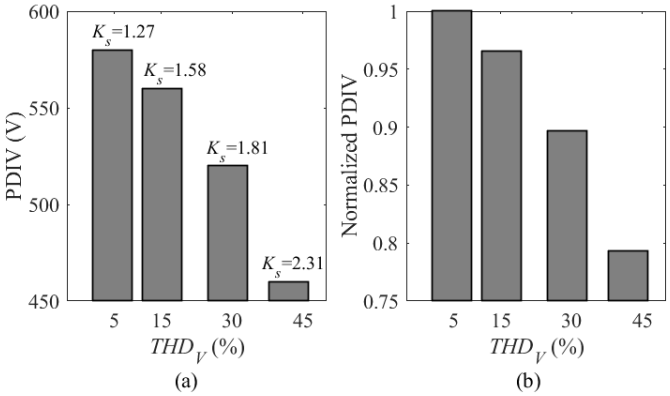

Fig. 6. (a) *PDIV and* ***(b)*** *Normalized PDIV calculated at different levels of THD_V*

5.2. Online Partial Discharge Diagnostics

The online PD measurements are conducted at different levels of voltage harmonics produced in VFD-fed EMs, and results are presented in Fig. 7. For each THD_V level, the test is conducted 10 times and the trigger level for all the measurements is adjusted as 10 pC. Based on the PD sweep signal captured for reference time (T_r) equal to 20 ms, PD activity is investigated by calculating the average PD pulse amplitude (q_i) and pulse repetition rate (m).

In the beginning, the VFD-fed EMs are operated at designed speed (e.g. equal to 100%), and PD measurements are carried out at nearly sinusoidal waveform of the applied voltage $THD_V = 4.61\%$ and $K_s = 1.27$, the results are outlined in Figure 7(a). From Fig. 7(a), at minimum values of THD_V and K_s, both q_i and m determined from the captures PD signals are also minimum. For T_r equal to 20 ms, only a few PD pulses (30 s^{-1}) with noticeable values of q_i (0.047 nC) are observed.

The operating speed of VFD-fed EMs is gradually reduced to 71%, 22% and 5%, and PD measurements are carried out at higher levels of THD_V and K_s. Figs. 7(b), 7(c), and 7(d) present the PD measurements carried out at THD_V and K_s levels up to 15.17% and 1.58, 29.06% and 1.81, and 41.94%, and 2.31, respectively. From Fig. 7(b), it can be observed that both q_i and m evaluated at 15.17% THD_V and

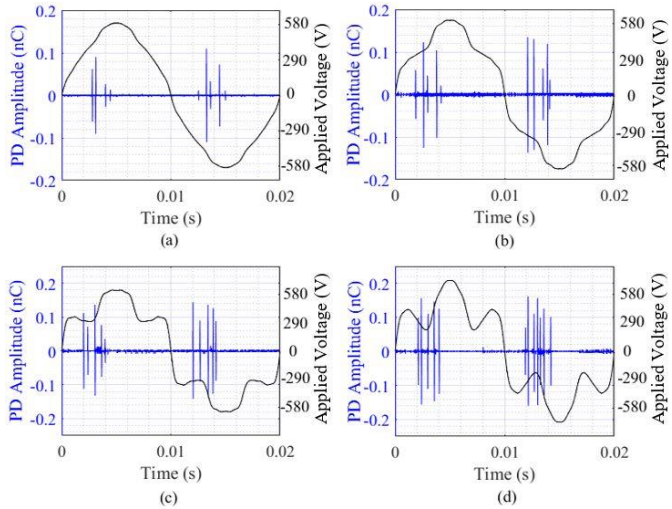

Fig. 7. *PD activity captured at various THD_V and K_s levels* ***(a)*** *4.61% and 1.27,* ***(b)*** *15.17% and 1.58,* ***(c)*** *29.06% and 1.81, and* ***(d)*** *41.94%, and 2.31, respectively.*

1.58 K_s are (50 s^{-1}) and (0.0611 nC), slightly higher than the both values observed in Fig. 7(a). Similarly, that both q_i and m evaluated at 29.06% THD_V and 1.81 K_s and are (55s^{-1}) and (0.102nC), as witnessed in Fig. 7(c). At 41.94% THD_V and 2.31 K_s, PD signals captured for 20 ms contain the highest values of both m and q_i (e.g. 60 s^{-1} and 0.12 nC), respectively. Therefore, by increasing THD_V (from 4.61% to 41.94%) and K_s (from 1.27 to 2.31), both m and q_i increased upto 100% and 155%, respectively.

5.3. Evaluation of PD Characteristic Features

At different levels of voltage harmonic distortion, the PD characteristic features including q_a, I, P, and D are evaluated, results are depicted in Fig. 8. From Fig. 8, it can be inferred that the increase in the level of voltage harmonic distortion causes a significant increase in PD characteristic features. For instance, the increase in THD_V level from 4.61% to 41.94% and K_s level from 1.27 to 2.31 cause an increase in q_a up to 4.3 times, I up to 4.5 times, P up to 4.9 times, and D up to 5.1 times. Therefore, it can be inferred that the increase in PD characteristic features at high level of voltage distortion amplified the PD severity level, and ultimately, the risk of insulation failure in VFD-fed EMs is increased.

5.4. Discussions

The introduction of harmonic components in the applied voltage waveform leads to a noticeable increase in PD activity (e.g. PDIV decreases and the values of PD characteristic features increase). This alteration in PD behavior when VFD-fed EMs are operated can be explained in three different ways.

In first way, the addition of harmonic components to the applied voltage increases the peak amplitude of the voltage waveform, resulting in extended PD activity at higher voltage amplitudes.

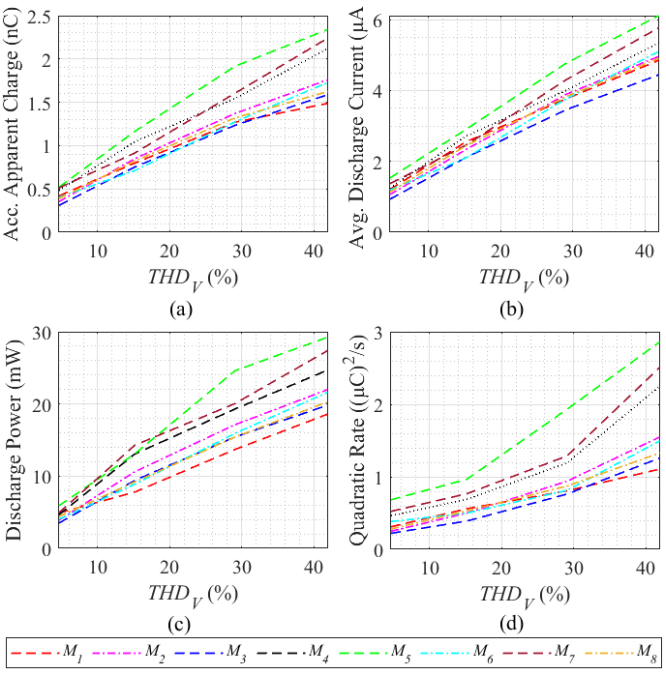

Fig. 8. *PD characteristic features identified for eight VFD-fed EMs under a range of voltage harmonic distortion* ***(a)*** q_a, ***(b)*** *I,* ***(c)*** *P, and* ***(d)*** *D*

The decrease in the operating speed of VFD-fed EM leads to the addition of current harmonic distortion in the sinusoidal current waveform. This, in turn, raises the stator winding temperature. When at higher temperatures, electrons absorb thermal energy, reduces the relative air density of electrons, this leads to increase the electron mean free path. Therefore, the electrons absorb more energy and travel a greater distance between two collisions, leading to electric discharge.

In third way, when the harmonic distortion of the applied voltage waveform is increased, the equilibrium temperature of the stator winding in EMs rises [23], reducing the amount of energy that needs to be supplied by bombarding electrons. This makes PD more energetic and powerful at high values of voltage harmonics.

6. ESTIMATION OF PARTIAL DISCHARGE SEVERITY

PD severity in VFD-fed EMs can be estimated based on the PD characteristic features (e.g. q_a, I, P, and D) evaluated at a certain voltage harmonic distortion level. To do this, various probability distribution functions are used to create probability density functions (PDFs) and cumulative distribution functions (CDFs) with the PD characteristic features data at different voltage harmonic distortion levels. At a specific harmonic level, 350 data samples of PD sweep signal were captured and corresponding values of q_a, I, P, and D are determined. The PD measurements are ignored for PD amplitude values lower than 10 pC. Accordingly, PDF and CDF using probability distribution functions (e.g. Normal, Rayleigh, Weibull, Gamma, and Generalized extreme value (GEV) are employed for the fitting of PD data. For instance, Fig. 9 presents the plot of PDF and CDF for data fitting of q_a, I, P, and D at 4.61% THD_V and 1.27 K_s. An appropriate distribution function is discovered by employing the distribution fitting tools.

The Generalized extreme value (GEV) distribution, introduced by Jenkinson in 1955, is used to describe the probability distribution function of standardized maxima or minima. The GEV distribution is a three-parameter function, consisting of shape parameter (ξ), location parameter (μ), and scale parameter (σ). Based on the shape parameter (ξ), GEV probability distribution family is further divided into three types such as Weibull distribution when $\xi < 0$, Freshet distribution when $\xi > 0$, and Gumbel distribution when $\xi = 0$ [24].

The R-squared (R^2) goodness-of-fit hypothesis is conducted to determine which of the five probability distribution functions best fit the PD characteristic features. The results of this hypothesis are presented in Table 2, and it is found that GEV yields the highest coefficient of determination in three out of four PD characteristic features. Consequently, GEV was chosen to estimate the probability of PD activity under voltage harmonic concentration.

Using three parameters GEV distribution function, PDF for PD characteristic features is given by (12) [25].

$$f(x) = \frac{1}{\sigma}(1+\mathfrak{F}x)^{\frac{-1}{\mathfrak{F}}-1}\exp -(1+\mathfrak{F}x)^{\frac{-1}{\mathfrak{F}}} \qquad (12)$$

where

$$x = \frac{z-\mu}{\sigma}, x > \mu - \frac{\sigma}{\mathfrak{F}} \text{ for } \mathfrak{F} > 0 \qquad (13)$$

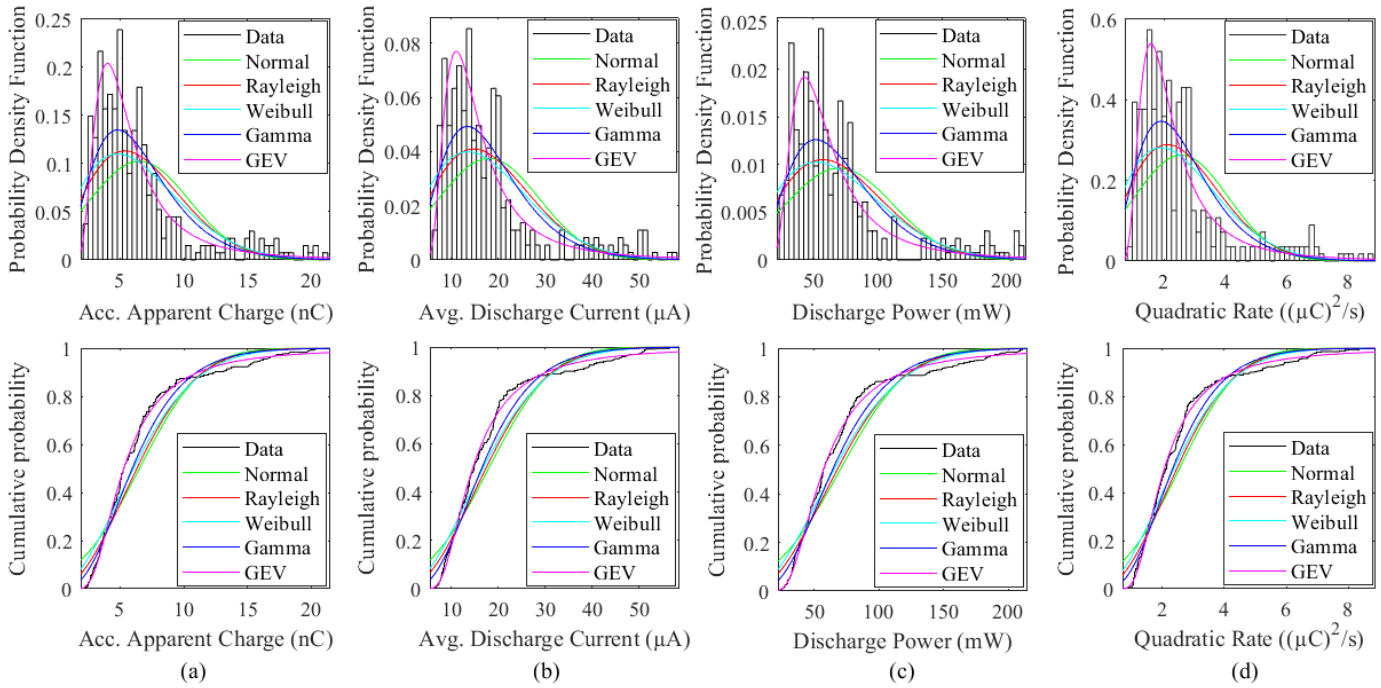

Fig. 9. *Example of PDF and CDF for data fitting of PD features at 4.61% THD_V and 1.27 K_s* ***(a)*** *q_a,* ***(b)*** *I ,* ***(c)*** *P, and* ***(d)*** *D*

Table 2 Results of r-square hypothesis test (coefficient of determination)

PD feature	Normal	Rayleigh	Weibull	Gamma	GEV
q_a	0.6752	0.6997	0.7265	0.7817	0.9654
I	0.6617	0.6698	0.6919	0.7854	0.9612
P	0.6742	0.7141	0.7401	0.7765	0.9599
D	0.6887	0.7021	0.7511	0.7656	0.9432

where

$$x = \frac{z-\mu}{\sigma}, x > \mu - \frac{\sigma}{\mathfrak{F}} \text{ for } \mathfrak{F} > 0 \quad (13)$$

By integrating (12), the CDF $P_c(x; \xi)$ is given in (13):

$$P_c(x;\xi) = \exp - (1+\mathfrak{F}x)^{\frac{-1}{\mathfrak{F}}} \quad (13)$$

For estimating the PD severity at a specific voltage harmonic distortion level, the PD characteristic features estimated at almost sinusoidal voltage waveform (4.61% THD_v and 1.27 K_s) are taken as the reference values (e.g. $q_{a,ref}$, I_{ref}, P_{ref}, and D_{ref}). Therefore, the probability of occurrence ($P_o(x)$) of PD characteristic features (e.g. q_a, I, P, and D), that characterizes the PD severity, at a specific harmonic level greater than or equal to the PD characteristic features (I_{ref}, $q_{a,ref}$, D_{ref}, and P_{ref}) estimated at 4.61% THD_v and 1.27 K_s is given by

$$P_o(x) = 1 - P_c(x;\xi) \quad (14)$$

Considering the combined influence of four PD characteristic features (e.g. q_a, I, P, and D), the average probability of occurrence of PD activity ($P_{o,a}$) at a specific voltage harmonics level is calculated using linearly distributed PD characteristic features:

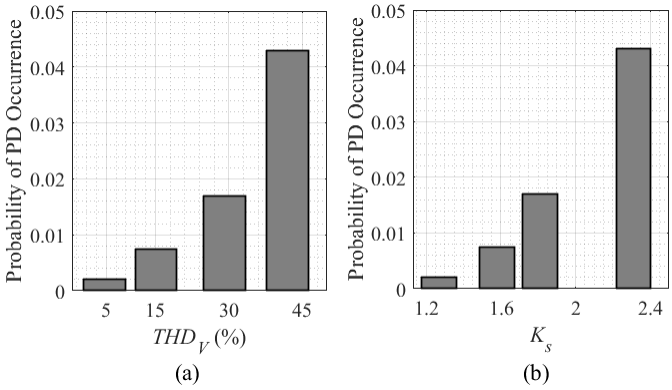

Fig. 10. *Estimated likelihood of PD activity occurring under different harmonic compositions*

$$P_{o,a} = q_{a,N}\frac{P_o(q_a)}{4} + I_N\frac{P_o(I)}{4} + P_N\frac{P_o(P)}{4} + D_N\frac{P_o(D)}{4} \quad (15)$$

where $q_{a,N}$, I_N, P_N, and D_N, represent the normalized values of I, q_a, D, and P calculated by (11). $P_o(I)$, $P_o(q_a)$, $P_o(D)$, and $P_o(P)$ represent the corresponding probability of occurrence of q_a, I, P, and D at specific harmonics level. Fig. 10 presents the $P_{o,a}$ calculated at different levels of voltage harmonic distortion. From Fig. 10, it was found that the increase in THD_V and K_s levels significantly increases the $P_{o,a}$, and PD severity in VFD-fed EMs is also increased.

Based on the estimated probability of occurrence of PD activity under different harmonic components, the assessment of PD severity is made by defining four different classes, as presented in Table 3. From Table 3, the severity levels are classified into negligible, low, medium, and high.

Based on the propsoed framework, asset managers can take remedial actions and schedule regular maintenace activities to ensure the healthy operation of VFD-fed EMs during voltage harmonic distortion. For instance, asset

Table 3 Probability ranges and severity classes

Level	Probability range	Severity Class	Definition
1. Negligible	$P_f \leq 10^{-3}$	Normal	No serious discharge occurs (Initial PD stage)
2. Low	$10^{-3} < P_f \leq 5^{-3}$	Attention	Weak discharge pulses appear
3. Medium	$5^{-3} < P_f \leq 5^{-1}$	Serious	PD pulses with significantly high amplitude appear
4. High	$P_f \geq 5^{-1}$	Pre-breakdown	PD pulses with very high amplitude appear

managers may follow the routine maintenance activities when PD severity level is negligible. Further increase in the PD severity from negligible to low level, the routine/ normal maintenance period may be decreased. When PD severity is increased to medium level, EM is taken under observation. With further increase in the PD severity level from medium to high, a complete inspection of VFD-fed EM by a human expert is necessary to replace the required components. Furthermore, the increase in PD severity due to voltage harmonic components can be avoided either mitigating the harmonic components or implementing an optimum operation of VFD-fed EMs [4].

7. CONCLUSIONS

This research investigated the effects of voltage harmonic distortion produced due to variable speed operation of VFD-fed EMs for estimating the PD severity. The results suggested that the harmonic distortion has a significant impact on PD severity, making reliable operation of VFD-fed EMs a challenge. The harmonic distortion parameters of the voltage waveform, K_s and THD_V, increased from 1.27 to 2.31 and 4.61% to 41.94%, respectively, during the experiments. These changes resulted in an increase in the values of PD characteristic features (q_a, I, P, D, and m) to 4.3 times, 4.5 times, 4.9 times, 5.1 times, and 2 times, respectively. These increases in PD characteristic parameters lead to an increased PD severity level and, consequently, a higher risk of insulation failure. Therefore, it is essential to have a thorough understanding of harmonic content in order to properly assess the effect of PD activity on insulation health and avoid any misinterpretations of PD data.

By applying five different probability distribution functions, the likelihood of PD activity and its severity at different voltage harmonic levels are calculated. The R-squared goodness-of-fit hypothesis is applied to investigate which of the five probability distribution functions is most suitable for fitting the PD characteristic features. The results of the hypothesis, with GEV having the highest coefficient of determination for three out of four PD characteristics. Consequently, GEV is utilized to estimate the probability of PD activity under voltage harmonic concentration.

This technique can be used to plan maintenance and replacement activities, ensuring a reliable level of performance for industrial applications that experience voltage harmonic distortion.

AUTHOR CONTRIBUTIONS

Waqar Hassan: Conceptualization; Data curation; Formal analysis; Investigation; Methodology; Resources; Writing – original draft. Muhammad Akmal: Formal analysis; Investigation; Methodology; Supervision; Writing – review & editing. Ghulam Amjad Hussain: Methodology; Resources; Supervision; Writing – review & editing. Ali Raza: Methodology; Resources; Writing – review & editing. Muhammad Shafiq: Supervision; Validation; Writing – review & editing.

CONFLICT OF INTEREST STATEMENT

The authors declare no conflict of interest.

FUNDING INFORMATION

This paper has not received any public funding.

DATA AVAILABILITY STATEMENT

The data that support the findings of this study are available from the first or corresponding author upon reasonable request.

ORCID

Waqar Hassan: https://orcid.org/0000-0003-4115-9408
Muhammad Akmal: https://orcid.org/0000-0002-3498-4146
Ghulam A. Hussain: https://orcid.org/0000-0002-5161-7233
Ali Raza: https://orcid.org/0000-0003-0947-3616
Muhammad Shafiq: https://orcid.org/0000-0002-2272-0899

REFERENCES

[1] A. Hughes and W. Drury, *Electric motors and drives: fundamentals, types and applications*. Newnes, 2013.

[2] G. C. Stone, H. G. Sedding, and C. Chan, "Experience With Online Partial-Discharge Measurement in High-Voltage Inverter-Fed Motors," *IEEE Transactions on Industry Applications*, vol. 54, no. 1, pp. 866-872, 2018.

[3] Y. Wang, T. Balachandran, Y. Hoole, Y. Yin, and K. S. Haran, "Partial discharge investigation of form-wound electric machine winding for electric aircraft propulsion," *IEEE Transactions on Transportation Electrification*, vol. 6, no. 4, pp. 1638-1647, 2020.

[4] W. Hassan, F. Mahmood, M. Akmal, and M. Nasir, "Optimum operation of low voltage variable-frequency drives to improve the performance of heating, ventilation, and air conditioning chiller system," *International Transactions on Electrical Energy Systems*, vol. 30, no. 9, p. e12481, 2020.

[5] W. Hassan, F. Mahmood, A. Andreotti, M. Pagano, and F. Ahmad, "Influence of Voltage Harmonics on Partial Discharge Diagnostics in Electric Motors Fed by Variable-Frequency Drives," *IEEE Transactions on Industrial Electronics,* vol. 69, no. 10, pp. 10605-10614, 2021.

[6] G. Bucci, F. Ciancetta, E. Fiorucci, and A. Ometto, "Uncertainty issues in direct and indirect efficiency determination for three-phase induction motors: remarks about the IEC 60034-2-1 standard," *IEEE Transactions on Instrumentation and Measurement,* vol. 65, no. 12, pp. 2701-2716, 2016.

[7] W. Koltunowicz *et al.*, "Evaluation of Stator Winding Insulation Using a Synchronous Multi-Channel PD Technique," *IEEE Transactions on Dielectrics and Electrical Insulation,* vol. 27, no. 6, pp. 1889-1897, 2020.

[8] R. E. Machines, "Off-line partial discharge measurements on the winding insulation," IEC 60034-27-1 Standard, CD, 2017.

[9] I. 60034-27-2, "Rotating electrical machines-Part 27-2: On-line partial discharge measurements on the stator winding insulation of rotating electrical machines," *International Electrotechnical Commission,* 2012.

[10] P. Wang, G. C. Montanari, and A. Cavallini, "Partial discharge phenomenology and induced aging behavior in rotating machines controlled by power electronics," *IEEE Transactions on Industrial Electronics,* vol. 61, no. 12, pp. 7105-7112, 2014.

[11] G. C. Montanari and P. Seri, "A partial discharge–based health index for rotating machine condition evaluation," *IEEE Electrical Insulation Magazine,* vol. 34, no. 2, pp. 17-23, 2018.

[12] K. K.-f. Yuen and H. S.-h. Chung, "Use of synchronous modulation to recover energy gained from matching long cable in inverter-fed motor drives," *IEEE transactions on power electronics,* vol. 29, no. 2, pp. 883-893, 2013.

[13] A. T. de Almeida, F. J. Ferreira, and D. Both, "Technical and economical considerations in the application of variable-speed drives with electric motor systems," *IEEE Transactions on Industry Applications,* vol. 41, no. 1, pp. 188-199, 2005.

[14] T. Billard, T. Lebey, and F. Fresnet, "Partial discharge in electric motor fed by a PWM inverter: off-line and on-line detection," *IEEE Transactions on Dielectrics and Electrical Insulation,* vol. 21, no. 3, pp. 1235-1242, 2014.

[15] M. Florkowski, B. Florkowska, J. Furgał, and P. Zydron, "Impact of high voltage harmonics on interpretation of partial discharge patterns," *IEEE Transactions on Dielectrics and Electrical Insulation,* vol. 20, no. 6, pp. 2009-2016, 2013.

[16] S. Bahadoorsingh and S. Rowland, "Investigating the impact of harmonics on the breakdown of epoxy resin through electrical tree growth," *IEEE Transactions on Dielectrics and Electrical Insulation,* vol. 17, no. 5, pp. 1576-1584, 2010.

[17] G. C. Montanari and P. Seri, "The effect of inverter characteristics on partial discharge and life behavior of wire insulation," *IEEE Electrical Insulation Magazine,* vol. 34, no. 2, pp. 32-39, 2018.

[18] I. Standard, "High-voltage test techniques: partial discharge measurements," *IEC-60270,* pp. 13-31, 2000.

[19] R. Langella, A. Testa, and E. Alii, "IEEE recommended practice and requirements for harmonic control in electric power systems," *University of Campania "Luigi Vanvitelli": Caserta, Italy,* 2014.

[20] W. Hassan, G. A. Hussain, F. Mahmood, S. Amin, and M. Lehtonen, "Effects of Environmental Factors on Partial Discharge Activity and Estimation of Insulation Lifetime in Electrical Machines," *IEEE Access,* 2020.

[21] I. F II, "IEEE recommended practices and requirements for harmonic control in electrical power systems," *New York, NY, USA,* pp. 1-1, 1993.

[22] V. M. Catterson, S. Bahadoorsingh, S. Rudd, S. D. McArthur, and S. M. Rowland, "Identifying harmonic attributes from online partial discharge data," *IEEE Transactions on Power Delivery,* vol. 26, no. 3, pp. 1811-1819, 2011.

[23] W. Hassan, G. A. Hussain, F. Mahmood, and M. Akmal, "Quantifying the Probability of Partial Discharge in VFD Fed Electric Motors under Voltage Harmonics Concentration," in *2022 20th International Conference on Harmonics & Quality of Power (ICHQP)*, 2022: IEEE, pp. 1-6.

[24] A. Bücher and J. Segers, "On the maximum likelihood estimator for the generalized extreme-value distribution," *Extremes,* vol. 20, no. 4, pp. 839-872, 2017.

[25] M. Pinheiro and R. Grotjahn, "An introduction to extreme value statistics," ed, 2015.